


Entangling two microwave modes via optomechanics

Qizhi Cai ¹, Jinkun Liao,^{1,*} and Qiang Zhou^{1,2}

¹*School of Optoelectronic Science and Engineering, University of Electronic Science and Technology of China, Chengdu, Sichuan, China*

²*Institute of Fundamental and Frontier Sciences, University of Electronic Science and Technology of China, Chengdu, Sichuan, China*



(Received 7 August 2019; published 29 October 2019)

We in theory proposed a hybrid system consisting of a mechanical resonator, an optical Fabry-Pérot cavity, and two superconducting microwave circuits to generate stationary continuous-variable quantum entanglement between two microwave modes. We show that the hybrid system can also achieve quantum entanglement of other bipartite subsystems in experimentally accessible parameter regimes, which has the potential to be useful in quantum information processing and quantum illumination radar.

DOI: [10.1103/PhysRevA.100.042330](https://doi.org/10.1103/PhysRevA.100.042330)

I. INTRODUCTION

As a particular resource of the quantum world, entanglement plays an important role in fundamental quantum mechanics and high-speed development of quantum technologies, such as quantum internet, quantum communication, quantum sensing, and quantum computers [1–5]. The realization of the above techniques must rely on the generation and distribution of entanglement between different quantum systems, including atoms, spins, photons, ions, phonons, and superconducting circuits [6–12].

Owing to the strong coupling with an external microwave field, superconducting circuits can control, store, and read the quantum information robustly with good scalability, which makes it a promising candidate for the physical implementation of quantum computers. Moreover, entangled microwaves can be used in quantum-enhanced radar schemes, namely, quantum illumination radar protocols, which utilize quantum resources to detect targets with low reflectivity hidden in a strong thermal noise bath. In the case where quantum entanglement is destroyed, its detection ability can still maintain quantum superiority, namely, exceeding the classical counterpart protocols [13–15]. Nowadays, realization of the prototype quantum radar has begun to land the ground in the microwave band, and it shows robustness to the ambient background noise and loss, which means it may have broad application prospects [16,17]. The above series of requirements and others make the generation of entangled microwaves and the distribution of their entanglement become research hotspots, and various theoretical schemes and physical experiments to realize entanglement between microwaves have emerged one after another in recent years [18–21].

In this work, we propose a theoretical scheme to achieve the entanglement of two microwave modes mediated by optomechanics. This hybrid quantum system consists of a mechanical resonator, two superconducting circuits, and an Fabry-Pérot optical cavity. It could be realized with the help of a lumped-element superconducting circuit, with a

freestanding mechanical membrane acting as drum-head capacitor which is capacitively coupled to two microwave cavities simultaneously (see Fig. 1). The drum-head capacitor could be optically coated to form a Fabry-Pérot optical cavity with the other side of the micromirror. Therefore, the vibrating drum-head mechanical membrane could capacitively interface with two microwave cavities at the same time while the optical intracavity mode is coupled with the drum head by the radiation pressure.

This quadripartite optoelectromechanical system has the potential to be used in quantum computer and quantum communication networks and quantum illumination radar systems. The optical intracavity mode is not susceptible to thermal noise, so it could be used as a flying qubit to interface with other distant nodes via fibers. The quantum entanglement between microwaves, light, and microwave could be distributed to other network nodes through the entanglement swapping protocol [22–25]. In addition, this quadripartite system can be fabricated on chips [26–28], which proposes a new approach to realize an integrated microwave source for quantum illumination radar systems.

This paper is organized as follows. Section II shows the basic physical model. The quantum Langevin equations with their linearization for describing the dynamics of the hybrid system are discussed in Sec. III. In Sec. IV we will derive the correlated matrix of the quantum fluctuation of the system to obtain the logarithmic negativity, which is considered as the entanglement measure in this work. In Sec. V we study the effects of different parameters on the quantum entanglement between microwave modes and also analyze the entanglement between other bipartite subsystems, such as light-microwave subsystems and so on, while Sec. VI is for the Conclusion.

II. MODEL

The proposed scheme is depicted in Fig. 1. On the one hand, the mechanical resonator with resonate frequency ω_m is capacitively coupled to two superconducting circuits simultaneously, with the two superconducting circuits with resonate frequency ω_{w1} , ω_{w2} , respectively. On the other hand, the mechanical resonator is coupled to a Fabry-Pérot optical

*jkliao@uestc.edu.cn

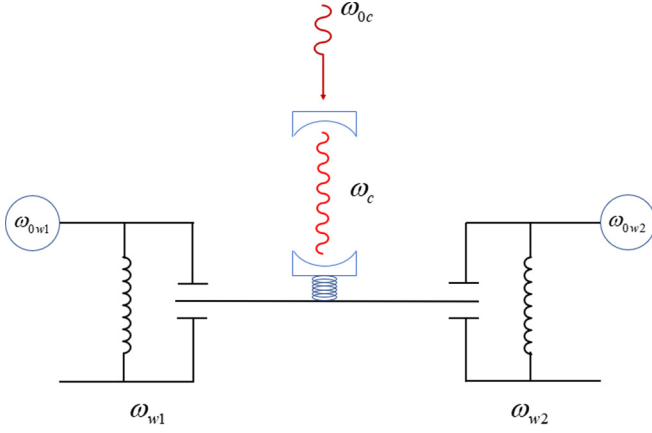


FIG. 1. Simple schematic diagram of the hybrid system.

cavity with resonate frequency ω_c . The optical and microwave cavities are driven at the frequencies $\omega_{0c} = \omega_c - \Delta_{0c}$, $\omega_{0w1} = \omega_{w1} - \Delta_{0w1}$, and $\omega_{0w2} = \omega_{w2} - \Delta_{0w2}$, respectively. The effective Hamiltonian for the quadripartite system is [29–31]

$$H = \frac{\hat{p}_x^2}{2m} + \frac{m\omega_m^2 \hat{x}^2}{2} + \frac{\hat{\Phi}_1^2}{2L_1} + \frac{\hat{Q}_1^2}{2[C_1 + C_{d1}(x)]} - e_1(t)\hat{Q}_1 + \frac{\hat{\Phi}_2^2}{2L_2} + \frac{\hat{Q}_2^2}{2[C_2 + C_{d2}(x)]} - e_2(t)\hat{Q}_2 + \hbar\omega_c \hat{a}^\dagger \hat{a} - \hbar G_{0c} \hat{a}^\dagger \hat{x} + i\hbar E_c (\hat{a}^\dagger e^{-i\omega_c t} - \hat{a} e^{i\omega_c t}), \quad (1)$$

where (\hat{x}, \hat{p}_x) are the canonical position and momentum of a mechanical resonator, $(\hat{\Phi}_j, \hat{Q}_j)$ are the canonical coordinates for the two microwave cavities ($j = 1, 2$ is a notation for the two superconducting microwave circuits), indicating the flux through equivalent inductors L_j and the charge on equivalent capacitors C_j , respectively. $(\hat{a}, \hat{a}^\dagger)$ is the annihilation and creation operator of the optical cavity mode, which satisfies $[\hat{a}, \hat{a}^\dagger] = 1$, and $E_c = \sqrt{2P_c \kappa_c} / \hbar \omega_c$ is related to the laser input, where P_c is the power of the input laser and κ_c describes the damping rate of the optical cavity. $G_{0c} = (\omega_c/l)\sqrt{\hbar/m\omega_m}$ is the coupling between optical cavity and mechanical resonator, with l the length of the optical Fabry-Pérot cavity and m the effective mass of the mechanical mode. The coherent driving of the superconducting microwave cavities with damping rates κ_{wj} is given by the electric potential $e_j(t) = -i\sqrt{2\hbar\omega_{wj}L_j}E_{wj}(e^{i\omega_{wj}t} - e^{-i\omega_{wj}t})$, where $E_{wj} = \sqrt{2P_{wj}\kappa_{wj}/\hbar\omega_{wj}}$. The reason for the coupling between the mechanical resonator and microwave cavities is that the capacitances are functions of the resonator displacement, namely, $C_{dj}(x)$. We expand these functions around their equilibrium positions d_j for two superconducting microwave cavities, and then we have $C_{dj}(x) = C_{dj}[1 - x_j(t)/d_j]$. Expanding the capacitive energy as a Taylor series, we find to first order

$$\frac{\hat{Q}_j^2}{2[C_j + C_{dj}(x_j)]} = \frac{\hat{Q}_j^2}{2C_{\Sigma j}} - \frac{\mu_j}{2d_j C_{\Sigma j}} \hat{x}_j(t) \hat{Q}_j^2, \quad (2)$$

where $C_{\Sigma j} = C_j + C_{dj}$ and $\mu_j = C_{dj}/C_{\Sigma j}$. In this manner, the Hamiltonian of Eq. (1) can be reshaped in the terms of the annihilation and creation operators of the superconducting microwave cavities' field $(\hat{b}_j, \hat{b}_j^\dagger)$ and the dimensionless position

and momentum operators of the mechanical resonator (\hat{q}, \hat{p}) , which satisfy $[\hat{b}_j, \hat{b}_j^\dagger] = 1$ and $[\hat{q}, \hat{p}] = i$, as

$$H = \hbar\omega_c \hat{a}^\dagger \hat{a} + \hbar\omega_{w1} \hat{b}_1^\dagger \hat{b}_1 + \hbar\omega_{w2} \hat{b}_2^\dagger \hat{b}_2 + \frac{\hbar\omega_m}{2} (\hat{p}^2 + \hat{q}^2) - \frac{\hbar G_{0w1}}{2} \hat{q} (\hat{b}_1 + \hat{b}_1^\dagger)^2 - \frac{\hbar G_{0w2}}{2} \hat{q} (\hat{b}_2 + \hat{b}_2^\dagger)^2 - \hbar G_{0c} \hat{q} \hat{a}^\dagger \hat{a} - i\hbar E_{w1} (e^{i\omega_{w1}t} - e^{-i\omega_{w1}t}) (\hat{b}_1 + \hat{b}_1^\dagger) - i\hbar E_{w2} (e^{i\omega_{w2}t} - e^{-i\omega_{w2}t}) (\hat{b}_2 + \hat{b}_2^\dagger) + i\hbar E_c (\hat{a}^\dagger e^{-i\omega_c t} - \hat{a} e^{i\omega_c t}), \quad (3)$$

where

$$\hat{b}_j = \sqrt{\frac{\omega_{wj}L_j}{2\hbar}} \hat{Q}_j + \frac{i}{\sqrt{2\hbar\omega_{wj}L_j}} \hat{\Phi}_j, \quad (4)$$

$$\hat{q} = \sqrt{\frac{m\omega_m}{\hbar}} \hat{x}, \quad \hat{p} = \frac{\hat{p}_x}{\sqrt{\hbar m\omega_m}}, \quad (5)$$

$$G_{0wj} = \frac{\mu_j \omega_{wj}}{2d_j} \sqrt{\frac{\hbar}{m\omega_m}}. \quad (6)$$

Typically, $\omega_m \ll \omega_c, \omega_{wj}$, since the mechanical resonant frequency is approximately 10 MHz while the optical and microwave cavity resonant frequency are the order of 10 GHz and 100 THz, respectively. Therefore, it is convenient to move into the interaction picture with respect to $H_0 = \hbar\omega_c \hat{a}^\dagger \hat{a} + \hbar\omega_{w1} \hat{b}_1^\dagger \hat{b}_1 + \hbar\omega_{w2} \hat{b}_2^\dagger \hat{b}_2$, and neglect fast oscillating terms at $\pm 2\omega_c, \pm 2\omega_{wj}$. In this case, the corresponding Hamiltonian of the system becomes

$$H = \hbar\Delta_{0c} \hat{a}^\dagger \hat{a} + \hbar\Delta_{0w1} \hat{b}_1^\dagger \hat{b}_1 + \hbar\Delta_{0w2} \hat{b}_2^\dagger \hat{b}_2 + \frac{\hbar\omega_m}{2} (\hat{p}^2 + \hat{q}^2) - \hbar G_{0w1} \hat{q} \hat{b}_1^\dagger \hat{b}_1 - \hbar G_{0w2} \hat{q} \hat{b}_2^\dagger \hat{b}_2 - \hbar G_{0c} \hat{q} \hat{a}^\dagger \hat{a} - i\hbar E_{w1} (\hat{b}_1 - \hat{b}_1^\dagger) - i\hbar E_{w2} (\hat{b}_2 - \hat{b}_2^\dagger) + i\hbar E_c (\hat{a}^\dagger - \hat{a}). \quad (7)$$

III. QUANTUM LANGEVIN EQUATIONS AND THEIR LINEARIZATION

However, the system would inevitably interact with the surrounding environment, bringing damping and noise to affect each mode. We can describe them with the help of the quantum Langevin equation where the Heisenberg equations for the system operators is revised by inserting the corresponding damping and noise terms. In this way, the nonlinear quantum Langevin equations of the system are given by

$$\dot{\hat{q}} = \omega_m \hat{p}, \quad (8)$$

$$\dot{\hat{p}} = -\omega_m \hat{q} - \kappa_m \hat{p} + G_{0c} \hat{a}^\dagger \hat{a} + G_{0w1} \hat{b}_1^\dagger \hat{b}_1 + G_{0w2} \hat{b}_2^\dagger \hat{b}_2 + \xi, \quad (9)$$

$$\dot{\hat{a}} = -(i\Delta_{0c} + \kappa_c) \hat{a} + iG_{0c} \hat{q} \hat{a} + E_c + \sqrt{2\kappa_c} \hat{a}_{in}, \quad (10)$$

$$\dot{\hat{b}}_1 = -(i\Delta_{0w1} + \kappa_{w1}) \hat{b}_1 + iG_{0w1} \hat{q} \hat{b}_1 + E_{w1} + \sqrt{2\kappa_{w1}} \hat{b}_{in,1}, \quad (11)$$

$$\dot{\hat{b}}_2 = -(i\Delta_{0w2} + \kappa_{w2}) \hat{b}_2 + iG_{0w2} \hat{q} \hat{b}_2 + E_{w2} + \sqrt{2\kappa_{w2}} \hat{b}_{in,2}, \quad (12)$$

where \hat{a}_{in} and $\hat{b}_{\text{in},j}$ are the input noise terms of optical and microwave modes, respectively, which could be considered as zero-mean Gaussian processes, satisfying the following correlation [32]:

$$\langle \hat{a}_{\text{in}}(t) \hat{a}_{\text{in}}^\dagger(t') \rangle = [N(\omega_c) + 1] \delta(t - t'), \quad (13)$$

$$\langle \hat{a}_{\text{in}}^\dagger(t) \hat{a}_{\text{in}}(t') \rangle = N(\omega_c) \delta(t - t'), \quad (14)$$

$$\langle \hat{b}_{\text{in},j}(t) \hat{b}_{\text{in},j}^\dagger(t') \rangle = [N(\omega_{w_j}) + 1] \delta(t - t'), \quad (15)$$

$$\langle \hat{b}_{\text{in},j}^\dagger(t) \hat{b}_{\text{in},j}(t') \rangle = N(\omega_{w_j}) \delta(t - t'), \quad (16)$$

in which $N(\omega_c) = 1/[\exp(\hbar\omega_c/k_B T) - 1]$ and $N(\omega_{w_j}) = 1/[\exp(\hbar\omega_{w_j}/k_B T) - 1]$ are the mean thermal excitation numbers of optical and microwave fields, respectively, where k_B is the Boltzmann constant and T is the temperature of the surrounding environment. Since $\hbar\omega_c/k_B T \gg 1$ at optical frequencies, we can safely assume that $N(\omega_c) \rightarrow 0$, while $N(\omega_{w_j})$ cannot be ignored even at quite low temperatures. What is more, in Eq. (9), κ_m is the mechanical damping rate and $\xi(t)$ is the quantum Brownian noise acting on the mechanical resonator, with the correlation function [33]

$$\langle \xi(t) \xi(t') \rangle = \frac{\kappa_m}{\omega_m} \int \frac{d\omega}{2\pi} e^{-i\omega(t-t')} \omega \left[\coth\left(\frac{\hbar\omega}{2k_B T}\right) + 1 \right]. \quad (17)$$

$\xi(t)$ is not δ correlated obviously and therefore does not describe a Markovian process. But the mechanical quantum effects are achieved only for a high mechanical quality factor ($Q_m = \omega_m/\kappa_m \gg 1$); in this limit, $\xi(t)$ becomes δ correlated [34], i.e., $\langle \xi(t) \xi(t') + \xi(t') \xi(t) \rangle / 2 \approx \kappa_m (2\bar{n}_m + 1) \delta(t - t')$, where $\bar{n}_m = 1/[\exp(\hbar\omega_m/k_B T) - 1]$ is the mean thermal excitation number of the mechanical resonator, like the microwave and optical counterparts mentioned above.

In order to achieve stationary and robust entanglement in continuous-variable systems, we would like to choose a working point where the cavities are intensely driven. In this way, the intracavity fields are strong enough to do the following approximation: $\hat{a} = \alpha_s + \delta\hat{a}$, $\hat{b}_j = \beta_{js} + \delta\hat{b}_j$, $\hat{p} = p_s + \delta\hat{p}$, and $\hat{q} = q_s + \delta\hat{q}$, in which α_s , β_{js} , p_s , q_s and $\delta\hat{a}$, $\delta\hat{b}_j$, $\delta\hat{p}$, $\delta\hat{q}$ are the fixed semiclassical points and their quantum fluctuation around the semiclassical points of quadripartite system, respectively. Then we insert the above approximation into Eqs. (8)–(12) and let the derivatives be zero, getting the fixed points

$$p_s = 0, \quad (18)$$

$$q_s = \frac{G_{0c}|\alpha_s|^2 + G_{0w1}|\beta_{1s}|^2 + G_{0w2}|\beta_{2s}|^2}{\omega_m}, \quad (19)$$

$$\alpha_s = \frac{E_c}{\kappa_c + i\Delta_c}, \quad (20)$$

$$\beta_{js} = \frac{E_{wj}}{\kappa_{wj} + i\Delta_{wj}}, \quad (21)$$

where $\Delta_c = \Delta_{0c} - G_{0c}q_s$ and $\Delta_{wj} = \Delta_{0wj} - G_{0wj}q_s$ are the effective detunings of the optical and microwaves fields, respectively. As mentioned above, the optical and microwave

intracavity fields are intensely driven, namely, $|\alpha_s| \gg 1$ and $|\beta_{s,j}| \gg 1$; thus, we can securely linearized Eqs. (8)–(12) around the fixed semiclassical points and get the following linear quantum Langevin equations for the quantum fluctuations of the hybrid system:

$$\delta\dot{\hat{q}} = \omega_m \delta\hat{p}, \quad (22)$$

$$\begin{aligned} \delta\dot{\hat{p}} = & -\omega_m \delta\hat{q} - \kappa_m \delta\hat{p} + G_{0c} \alpha_s (\delta\hat{a}^\dagger + \delta\hat{a}) \\ & + G_{0w1} \beta_{1s} (\delta\hat{b}_1^\dagger + \delta\hat{b}_1) + G_{0w2} \beta_{2s} (\delta\hat{b}_2^\dagger + \delta\hat{b}_2) + \xi, \end{aligned} \quad (23)$$

$$\delta\dot{\hat{a}} = -(\kappa_c + i\Delta_c) \delta\hat{a} + iG_{0c} \alpha_s \delta\hat{q} + \sqrt{2\kappa_c} \hat{a}_{\text{in}}, \quad (24)$$

$$\delta\dot{\hat{b}}_1 = -(\kappa_{w1} + i\Delta_{w1}) \delta\hat{b}_1 + iG_{0w1} \beta_{1s} \delta\hat{q} + \sqrt{2\kappa_{w1}} \hat{b}_{\text{in},1}, \quad (25)$$

$$\delta\dot{\hat{b}}_2 = -(\kappa_{w2} + i\Delta_{w2}) \delta\hat{b}_2 + iG_{0w2} \beta_{2s} \delta\hat{q} + \sqrt{2\kappa_{w2}} \hat{b}_{\text{in},2}, \quad (26)$$

where we have chosen the appropriate reference phases for the three input optical and microwaves fields so that α_s and β_{js} can be taken as real and positive.

IV. CORRELATED MATRIX OF QUANTUM FLUCTUATIONS

The continuous-variable entanglement between the two microwave cavities is generated by the microwave cavities' interaction mediated by the optomechanical bipartite system, in other words, the quantum correlations between the quadratures of three intracavity fields and the position and momentum of the mechanical resonator. Based on this reason, it is favorable to introduce the fluctuation quadratures $\delta\hat{X}_c = (\delta\hat{a} + \delta\hat{a}^\dagger)/\sqrt{2}$ and $\delta\hat{Y}_c = (\delta\hat{a} - \delta\hat{a}^\dagger)/i\sqrt{2}$ for the optical field, and $\delta\hat{X}_{wj} = (\delta\hat{b}_j + \delta\hat{b}_j^\dagger)/\sqrt{2}$ and $\delta\hat{Y}_{wj} = (\delta\hat{b}_j - \delta\hat{b}_j^\dagger)/i\sqrt{2}$ for the two microwave fields. The corresponding input noise operators are $\hat{X}_{c,\text{in}} = (\delta\hat{a}_{\text{in}} + \delta\hat{a}_{\text{in}}^\dagger)/\sqrt{2}$, $\hat{Y}_{c,\text{in}} = (\delta\hat{a}_{\text{in}} - \delta\hat{a}_{\text{in}}^\dagger)/i\sqrt{2}$, $\hat{X}_{wj,\text{in}} = (\delta\hat{b}_{\text{in},j} + \delta\hat{b}_{\text{in},j}^\dagger)/\sqrt{2}$, and $\hat{Y}_{wj,\text{in}} = (\delta\hat{b}_{\text{in},j} - \delta\hat{b}_{\text{in},j}^\dagger)/i\sqrt{2}$. In this way, from Eqs. (22)–(26), the linearized quantum Langevin equations become

$$\delta\dot{\hat{q}} = \omega_m \delta\hat{p}, \quad (27)$$

$$\delta\dot{\hat{p}} = -\omega_m \delta\hat{q} - \kappa_m \delta\hat{p} + G_c \delta\hat{X}_c + G_{w1} \delta\hat{X}_{w1} + G_{w2} \delta\hat{X}_{w2} + \xi, \quad (28)$$

$$\delta\dot{\hat{X}}_c = -\kappa_c \delta\hat{X}_c + \Delta_c \delta\hat{Y}_c + \sqrt{2\kappa_c} \hat{X}_{c,\text{in}}, \quad (29)$$

$$\delta\dot{\hat{Y}}_c = -\kappa_c \delta\hat{Y}_c - \Delta_c \delta\hat{X}_c + G_c \delta\hat{q} + \sqrt{2\kappa_c} \hat{Y}_{c,\text{in}}, \quad (30)$$

$$\delta\dot{\hat{X}}_{w1} = -\kappa_{w1} \delta\hat{X}_{w1} + \Delta_{w1} \delta\hat{Y}_{w1} + \sqrt{2\kappa_{w1}} \hat{X}_{w1,\text{in}}, \quad (31)$$

$$\delta\dot{\hat{Y}}_{w1} = -\kappa_{w1} \delta\hat{Y}_{w1} - \Delta_{w1} \delta\hat{X}_{w1} + G_{w1} \delta\hat{q} + \sqrt{2\kappa_{w1}} \hat{Y}_{w1,\text{in}}, \quad (32)$$

$$\delta\dot{\hat{X}}_{w2} = -\kappa_{w2}\delta\hat{X}_{w2} + \Delta_{w2}\delta\hat{Y}_{w2} + \sqrt{2\kappa_{w2}}\hat{X}_{w2,\text{in}}, \quad (33)$$

$$\delta\dot{\hat{Y}}_{w2} = -\kappa_{w2}\delta\hat{Y}_{w2} - \Delta_{w2}\delta\hat{X}_{w2} + G_{w2}\delta\hat{q} + \sqrt{2\kappa_{w2}}\hat{Y}_{w2,\text{in}}, \quad (34)$$

where

$$G_{wj} = \sqrt{2}G_{0wj}\beta_{sj} = \frac{\mu_j\omega_{wj}}{d_j} \sqrt{\frac{P_{wj}\kappa_{wj}}{m\omega_m\omega_{0wj}(\kappa_{wj}^2 + \Delta_{wj}^2)}}, \quad (35)$$

$$A = \begin{pmatrix} 0 & \omega_m & 0 & 0 & 0 & 0 & 0 & 0 \\ -\omega_m & -\kappa_m & G_c & 0 & G_{w1} & 0 & G_{w2} & 0 \\ 0 & 0 & -\kappa_c & \Delta_c & 0 & 0 & 0 & 0 \\ G_c & 0 & -\Delta_c & -\kappa_c & 0 & 0 & 0 & 0 \\ 0 & 0 & 0 & 0 & -\kappa_{w1} & \Delta_{w1} & 0 & 0 \\ G_{w1} & 0 & 0 & 0 & -\Delta_{w1} & -\kappa_{w1} & 0 & 0 \\ 0 & 0 & 0 & 0 & 0 & 0 & -\kappa_{w2} & \Delta_{w2} \\ G_{w2} & 0 & 0 & 0 & 0 & 0 & -\Delta_{w2} & -\kappa_{w2} \end{pmatrix}, \quad (38)$$

and the solution of Eq. (37) is

$$v(t) = M(t)v(0) + \int_0^t ds M(s)n(s), \quad (39)$$

where $M(t) = \exp(At)$.

In order to test the stability of the hybrid system, we use the Routh-Hurwitz criterion [35,36]. If the real part of all eigenvalues of matrix A is negative, then we can assume that the system is stable and will approach a steady state. However, the explicit expression is too cumbersome, so we omit it here. With no special statement (Fig. 2 has), the parameters used in the numerical simulation for logarithmic negativity, i.e., entanglement, of the hybrid system will satisfy the Routh-Hurwitz criterion, that is, our numerical simulation is carried out under the condition that the system is always stable.

As we know, the quantum noise terms in Eq. (37) are zero-mean Gaussian and the dynamics are linear so that the steady state of the quantum fluctuations is a continuous-variable quadripartite Gaussian state, entirely characterized by the 8×8 correlation matrix. This matrix has components $V_{ij} = \langle u_i(\infty)u_j(\infty) + u_j(\infty)u_i(\infty) \rangle / 2$. When the system is stable, by using Eq. (39) we can get

$$V_{ij} = \sum_{k,l} \int_0^\infty ds \int_0^\infty ds' M(s)_{ik} M(s')_{jl} \Phi(s-s')_{kl}, \quad (40)$$

in which $\Phi_{kl}(s-s') = \langle n_k(s)n_l(s') + n_l(s')n_k(s) \rangle / 2$ is the matrix of stationary noise correlation functions. Here $\Phi_{kl}(s-s') = D_{kl}\delta(s-s')$, where $D = \text{diag}[0, \kappa_m(2\bar{n}_m + 1), \kappa_c, \kappa_c, \kappa_{w1}(2N(\omega_{w1}) + 1), \kappa_{w1}(2N(\omega_{w1}) + 1), \kappa_{w2}(2N(\omega_{w2}) + 1), \kappa_{w2}(2N(\omega_{w2}) + 1)]$ is an eight-dimensional diagonal

$$G_c = \sqrt{2}G_{0c}\alpha_s = \frac{2\omega_c}{L} \sqrt{\frac{P_c\kappa_c}{m\omega_m\omega_{0c}(\kappa_c^2 + \Delta_c^2)}}, \quad (36)$$

are the effective the electromechanical and optomechanical couplings, respectively. Equations (27)–(34) can be rewritten as a matrix form

$$\dot{v}(t) = Av(t) + n(t), \quad (37)$$

in which $v(t) = [\delta\hat{q}(t), \delta\hat{p}(t), \delta\hat{X}_c(t), \delta\hat{Y}_c(t), \delta\hat{X}_{w1}(t), \delta\hat{Y}_{w1}(t), \delta\hat{X}_{w2}(t), \delta\hat{Y}_{w2}(t)]^T$ (the notation T means matrix transpose), $n(t) = (0, \xi(t), \sqrt{2\kappa_c}\delta\hat{X}_{c,\text{in}}, \sqrt{2\kappa_c}\delta\hat{Y}_{c,\text{in}}, \sqrt{2\kappa_{w1}}\delta\hat{X}_{w1,\text{in}}, \sqrt{2\kappa_{w1}}\delta\hat{Y}_{w1,\text{in}}, \sqrt{2\kappa_{w2}}\delta\hat{X}_{w2,\text{in}}, \sqrt{2\kappa_{w2}}\delta\hat{Y}_{w2,\text{in}})^T$, and

matrix; in this way, Eq. (40) becomes

$$V = \int_0^\infty ds M(s)DM^T(s). \quad (41)$$

Under the condition that the system is stable $M(\infty) = 0$, by Lyapunov's first theorem [33], Eq. (41) is equivalent to

$$AV + VA^T = -D. \quad (42)$$

By solving Eq. (42), the 8×8 matrix V can be obtained. Then we can calculate the entanglement of the interested bipartite systems, like two superconducting microwave circuits, light-microwave subsystems, and so on, by tracing out the uninterested rows and columns of V . After this kind of operation, the induced correlation matrix of the interested bipartite system is a 4×4 matrix as follows:

$$V_{bi} = \begin{pmatrix} V_1 & V_3 \\ V_3^T & V_2 \end{pmatrix}. \quad (43)$$

Furthermore, we use the logarithmic negativity to quantify the entanglement of the interested bipartite system [37,38]

$$E_N = \max[0, -\ln 2\eta^-], \quad (44)$$

where $\eta^- \equiv 2^{-1/2}[\Sigma(V_{bi}) - \sqrt{\Sigma(V_{bi})^2 - 4 \det V_{bi}}]^{1/2}$ and $\Sigma(V_{bi}) \equiv \det V_1 + \det V_2 - 2 \det V_3$. The corresponding numerical simulation is discussed in the next section.

V. RESULTS

For the purpose of the hybrid system described herein, which can be realized by existing experimental approaches, the following simulation parameters are based on Refs. [39,40] and their feasible extension.

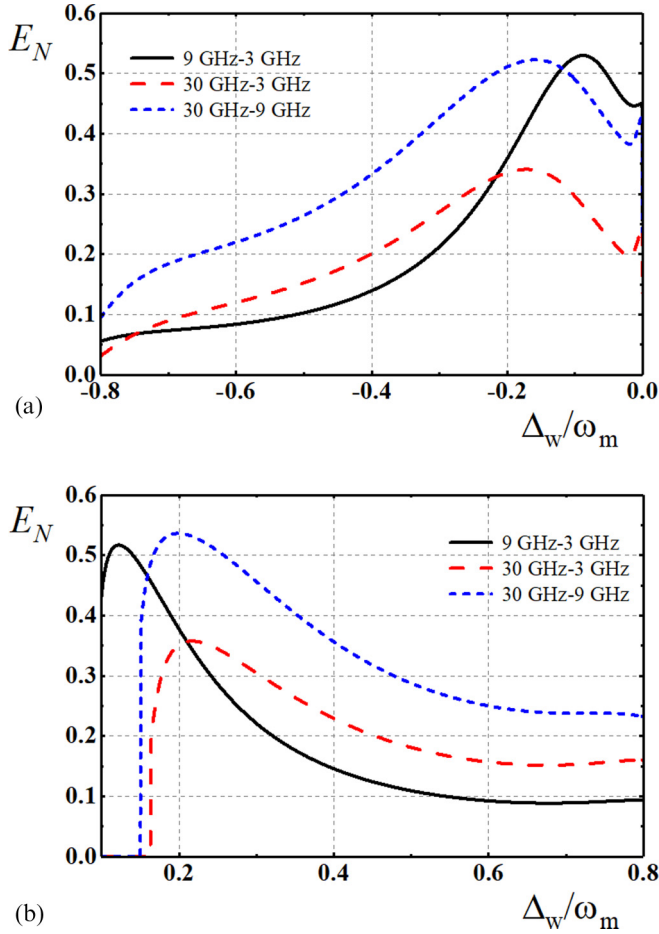


FIG. 2. Entanglement between two microwaves with different frequency. (Full black line: $\omega_{w1}/2\pi = 9$ GHz and $\omega_{w2}/2\pi = 3$ GHz. Dashed red line: $\omega_{w1}/2\pi = 30$ GHz and $\omega_{w2}/2\pi = 3$ GHz. Dotted blue line: $\omega_{w1}/2\pi = 30$ GHz and $\omega_{w2}/2\pi = 9$ GHz.) The surrounding temperature T is fixed at 15 mK, the optical detuning $\Delta_c = \omega_m$, while the other parameters are $\lambda_{0c} = 1550$ nm, $\kappa_c = 0.08 \omega_m$, $P_c = 30$ mW, $m = 10$ ng, $\omega_m/2\pi = 10$ MHz, $\kappa_{w1} = \kappa_{w2} = 0.02 \omega_m$, $P_{w1} = P_{w2} = 30$ mW, $d_1 = d_2 = 100$ nm, $\mu_1 = \mu_2 = 0.008$, and $\Delta_{w1} = -\Delta_{w2} \equiv \Delta_w$. (a) The microwave detuning range is from -0.8 to 0 Δ_w/ω_m , (b) The microwave detuning range is from 0.1 to 0.8 Δ_w/ω_m .

The simulation parameters are listed as follows. For the optical part, the driven laser wavelength $\lambda_{0c} = 1550$ nm, the damping rate $\kappa_c = 0.08 \omega_m$, the driving power $P_c = 30$ mW, and the length of the cavity $L = 1$ mm. For the mechanical part, the resonator mass $m = 10$ ng, the resonant frequency $\omega_m/2\pi = 10$ MHz, and its quality factor $Q = 5 \times 10^4$. For the microwave circuits part, we assume their damping rates $\kappa_{w1} = \kappa_{w2} = 0.02 \omega_m$, the input power $P_{w1} = P_{w2} = 30$ mW, the parameter related to the coupling $d_1 = d_2 = 100$ nm, and $\mu_1 = \mu_2 = 0.008$. The frequency of the two microwave circuits and the optical detuning Δ_c will show up in the bottom of the figures as well as the surrounding temperature. What is more, the microwave detunings are set to be opposite $\Delta_{w1} = -\Delta_{w2} \equiv \Delta_w$.

Figure 2 shows the entanglement between two different frequency microwave modes. We chose three pairs of microwave frequencies for simulation, 9–3 GHz, 30–3 GHz, 30–9 GHz.

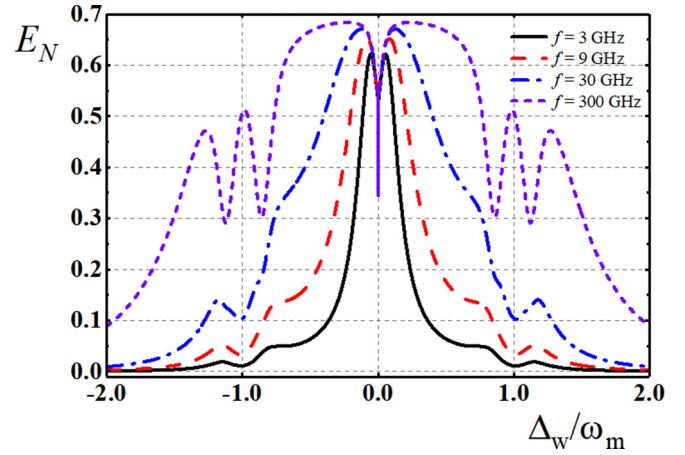


FIG. 3. Entanglement between two microwaves with the same frequency. (Full black line: $\omega_{w1}/2\pi = \omega_{w2}/2\pi = 3$ GHz. Dashed red line: $\omega_{w1}/2\pi = \omega_{w2}/2\pi = 9$ GHz. Dotted dash blue line: $\omega_{w1}/2\pi = \omega_{w2}/2\pi = 30$ GHz. Dotted purple line: $\omega_{w1}/2\pi = \omega_{w2}/2\pi = 300$ GHz.) The other parameters are the same as Fig. 2.

The biggest feature in Fig. 2 is that in an interval where the microwave detuning is larger than zero, the entanglement described by the three curves is abruptly going to zero, and for the beauty of the drawing, we blocked this part and divided it into two parts, respectively showing the characteristics of entanglement in the case where the microwave detuning is positive and negative. This is because the system does not satisfy the Routh-Hurwitz criterion in this interval, but the stationary and robust entanglement we discuss in this work is under the condition that the system is stable. If the system is unstable, the stationary and robust entanglement cannot be achieved. What is more, the width of these intervals varies with the frequencies of the entangled microwave pair, and the maximum entanglement is obtained on either side of the interval. There is a method to keep away from the adverse effects of the system instability caused by microwave tuning on the system; we chose the two microwave resonant frequencies to be the same. As we can see below, this can avoid the unstable situation and enable the system to be wideband tuned to adapt to a wider range of application scenarios.

The reason why we set the frequency of the two microwave cavities to be the same to avoid the instability of the system can be explained in mathematical form. As we can see above, the parameters of the two microwave cavities are set to be the same except for the resonant frequencies, and the two microwave detunings are the same value except for a minus sign. If two microwave resonant frequencies are same, the two microwave circuits behave like twin circuits because the structure parameters of two microwave circuits are completely the same. When we red-detune one microwave circuit, the other one is blue detuned and vice versa, which means under this condition the entanglement is an even function of the detuning, namely, the entanglement on the red sideband is symmetrical to the one on the blue sideband. With this idea, we chose the microwave frequencies to be the same and show their entanglement properties in Fig. 3.

As shown in Fig. 3, each curve is symmetrical based on the line of zero detuning, and the higher the frequency of the

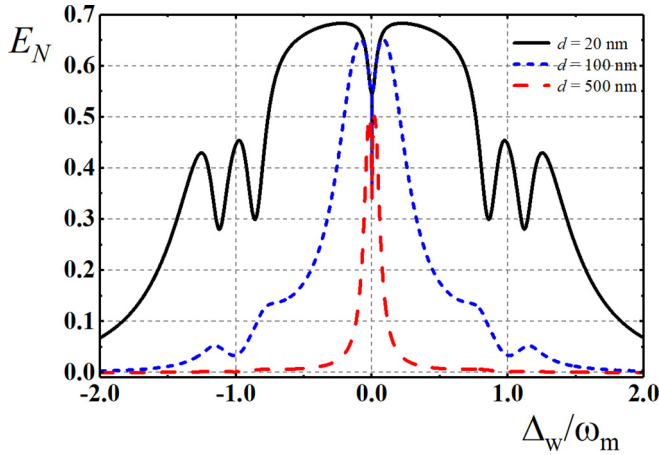


FIG. 4. Entanglement between two microwaves with the same frequency with different d . (Full black line: $d_1 = d_2 = 20$ nm. Dotted dash blue line: $d_1 = d_2 = 100$ nm. Dashed red line: $d_1 = d_2 = 500$ nm.) The microwave frequency $\omega_{w1}/2\pi = \omega_{w2}/2\pi = 9$ GHz. The other parameters are the same as Fig. 2.

selected microwave pair, the larger the entanglement between the two microwave modes, and the maximum entanglement is obtained near the zero detuning. At this time, the system instability will not occur during the microwave broadband tuning process, that is, the Routh-Hurwitz criterion is always satisfied.

Next, we study the effect of architecture parameters of the hybrid system on microwave entanglement. In Fig. 4, the smaller d_1 ($d_1 = d_2$) contributes the better entanglement at the same microwave frequency $\omega_{w1}/2\pi = \omega_{w2}/2\pi = 9$ GHz. This could be explained by Eq. (35). The two microwave circuits are connected by the interaction with the optomechanical subsystem, and the electromechanical couplings G_{wj} increase with the d_j decreases. When we increase the coupling G_{wj} of two microwave circuits to the optomechanical subsystem, it also indirectly enhances the coupling between the two microwave circuits, which enlarges the entanglement between them.

Figure 5 shows the entanglement of two microwave cavities versus the surrounding temperature at three pairs of different microwave frequencies: 3, 30, and 300 GHz, and the criterion of choosing the microwave detunings is to maximize entanglement. As Fig. 5 depicts, the higher the frequency of two microwave cavities, the better the temperature tolerance of entanglement between two microwaves. When the microwave frequency is selected to be 300 GHz, entanglement still exists above 10 K; this is because the microwave photon has higher energy and is more tenacious facing the thermal noise environment.

Now we turn to study the entanglement between light and microwaves in this hybrid system. As shown in Fig. 6, it is known that the optical detuning $\Delta_c = \omega_m$, and when $\Delta_c = \omega_m \approx \Delta_w$, the entanglement between light and microwave reaches its maximum, while the entanglement between other subsystems, such as mechanical resonator-microwave circuits, microwave circuits, and the other one, are compressed. This is because, in this case, the optical cavity and the microwave cavities are resonated through the optomechanical resonance

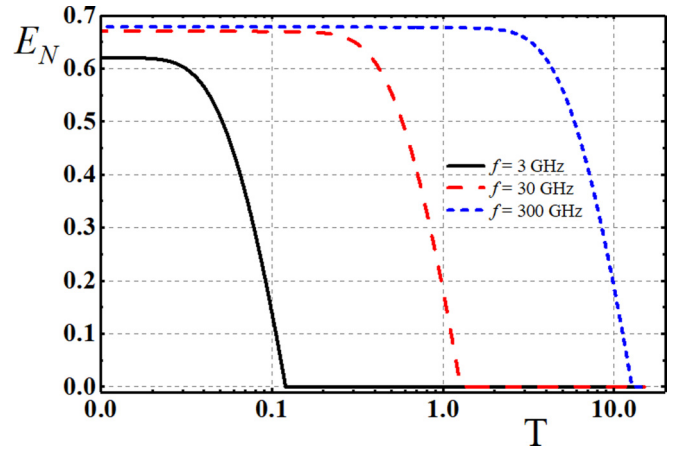


FIG. 5. Entanglement between two microwaves with different frequency for temperature. (Full black line: $\omega_{w1}/2\pi = \omega_{w2}/2\pi = 3$ GHz, $\Delta_w = -0.05\omega_m$. Dashed red line: $\omega_{w1}/2\pi = \omega_{w2}/2\pi = 30$ GHz, $\Delta_w = -0.12\omega_m$. Dotted blue line: $\omega_{w1}/2\pi = \omega_{w2}/2\pi = 300$ GHz, $\Delta_w = -0.13\omega_m$.) The other parameters are the same as Fig. 2.

and the electromechanical resonance, in other words, the entanglement between light and microwaves mediated by a mechanical resonator is at the expense of optomechanical and electromechanical entanglement.

In this section, we show the entanglement between two microwave circuits with different resonate frequencies, the influence of different parameters on the entanglement between two microwave modes with the same resonate frequency, and the entanglement of light and microwaves in the hybrid system. As shown in Fig. 2, though the stationary and robust entanglement between two microwave circuits with different frequencies cannot be achieved in a small microwave detuning interval, we could make the microwave detuning controlled in a small interval, like from -0.4 to -0.1 on the Δ_w/ω_m axis, and still obtain the stationary and robust entanglement, which has the potential to correlate different nodes in quantum computers, be they entangled microwave sources for quantum illumination radar sor other applications. From Figs. 3–5, we can know that increasing the coupling of the two microwave cavities can acquire the larger entanglement between two microwave modes, and raising the energy of microwaves can make the entanglement more tenacious in the thermal noise bath. Last but not least, Fig. 6 shows the entanglement between microwaves and light is at the expense of optomechanical and electromechanical entanglement. In this way, we can obtain the entanglement of different bipartite subsystems in the hybrid quadripartite system under different microwave detunings by changing the detuning of the microwave circuit. For example, we set the microwave detuning $\Delta_w = \pm\omega_m$, and the hybrid system now is used to generate the entanglement between light and microwave modes. Furthermore, we set the microwave detuning $\Delta_w = \pm 0.1\omega_m$ and the hybrid system now is used to generate the entanglement between two microwave modes.

Now let us briefly discuss the promising experimental approach to realize the hybrid quadripartite system. As mentioned in Ref. [40], a vibrating Si_3N_4 membrane coated

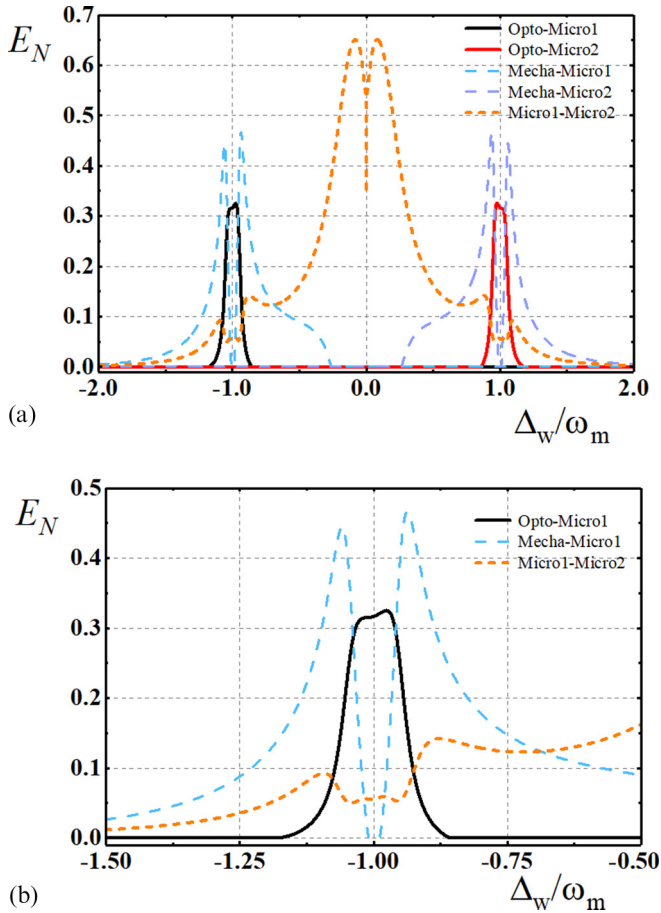


FIG. 6. The E_N plot for five bipartite subsystems. (Full red and black line: two subsystems consist of optical cavity and one of the microwave circuits. Dashed blue and purple line: two subsystems consist of mechanical resonator and one of the microwave circuits. Dotted orange line: the subsystem consist of two microwave circuits. “Opto” means optical cavity, “Micro1” and “Micro2” mean the two microwave cavities, and “Mecha” means the mechanical resonator.) (a) The full plot, and for clarity, (b) is a part of (a). $\omega_{w1}/2\pi = \omega_{w2}/2\pi = 9$ GHz, $\kappa_c = 0.01 \omega_m$, and the other parameters are the same as Fig. 2. (a) Full plot, the microwave detuning range is from -2 to 2 Δ_w/ω_m , (b) Partial plot, the microwave detuning range is from -1.5 to -0.5 Δ_w/ω_m .

in part with niobium interacts with an inductor-capacitor (LC) circuit that forms the microwave resonant cavity and couples by radiation pressure to an optically driven Fabry-Pérot cavity. Our scheme could be an extension of the scheme mentioned above; the niobium could coat on the two sides of the membrane and interact with two microwave circuits simultaneously, which builds the connection between the two microwave circuits with optomechanics.

VI. CONCLUSION

In this work, we theoretically proposed a scheme to build a hybrid system with the purpose of generating entanglement between two microwave modes, and the entanglement is measured by logarithmic negativity. The hybrid system consists of a Fabry-Pérot cavity, a mechanical resonator, and two superconducting microwave circuits. It not only can generate the entanglement between the two microwave modes, but also can realize the entanglement of interested bipartite subsystems in the system, such as light and microwave modes, microwave modes, microwave mode and mechanical resonator, and so on. Further, with different microwave detunings, the different bipartite subsystems of the hybrid system behave entangled. This means that we can choose proper microwave detuning to complete the requirements in the quantum information process, which microwave cavities are used to interface with solid-state qubits and light modes used for quantum communication, or act as an entangled microwave source to realize quantum illumination radar. Compared with previous theoretical work using logarithmic negativity as the measurement of entanglement [31,41–43], our maximum entanglement value E_N is larger, which means we can in theory realize more entanglement than their schemes.

ACKNOWLEDGMENTS

This work has been supported by the National Key R&D Program of China (No. 2018YFA0307400) and the National Natural Science Foundation of China (NSFC) (No. 61775025 and No. 91836102).

- [1] H. J. Kimble, The quantum internet, *Nature (London)* **453**, 1023 (2008).
- [2] S. Wehner, D. Elkouss, and R. Hanson, Quantum internet: A vision for the road ahead, *Science* **362**, eaam9288 (2018).
- [3] N. Gisin and R. Thew, Quantum communication, *Nat. Photonics* **1**, 165 (2007).
- [4] T. D. Ladd, F. Jelezko, R. Laflamme, Y. Nakamura, C. Monroe, and J. L. O’Brien, Quantum computers, *Nature (London)* **464**, 45 (2010).
- [5] C. L. Degen, F. Reinhard, and P. Cappellaro, Quantum sensing, *Rev. Mod. Phys.* **89**, 035002 (2017).
- [6] M. Saffman, T. G. Walker, and K. Mølmer, Quantum information with Rydberg atoms, *Rev. Mod. Phys.* **82**, 2313 (2010).
- [7] K. Hammerer, A. S. Sørensen, and E. S. Polzik, Quantum interface between light and atomic ensembles, *Rev. Mod. Phys.* **82**, 1041 (2010).
- [8] D. D. Awschalom, R. Hanson, J. Wrachtrup, and B. B. Zhou, Quantum technologies with optically interfaced solid-state spins, *Nat. Photonics* **12**, 516 (2018).
- [9] J.-W. Pan, Z.-B. Chen, C.-Y. Lu, H. Weinfurter, A. Zeilinger, and M. Ukowski, Multiphoton entanglement and interferometry, *Rev. Mod. Phys.* **84**, 777 (2012).
- [10] L.-M. Duan and C. Monroe, Quantum networks with trapped ions, *Rev. Mod. Phys.* **82**, 1209 (2010).
- [11] A. Bienfait, K. J. Satzinger, Y. P. Zhong, H.-S. Chang, M.-H. Chou, C. R. Conner, É. Dumur, J. Grebel, G. A. Peairs, R. G. Povey, and A. N. Cleland, Phonon-mediated quantum

- state transfer and remote qubit entanglement, *Science* **364**, 368 (2019).
- [12] Z.-L. Xiang, S. Ashhab, J. Q. You, and F. Nori, Hybrid quantum circuits: Superconducting circuits interacting with other quantum systems, *Rev. Mod. Phys.* **85**, 623 (2013).
- [13] S. Lloyd, Enhanced sensitivity of photodetection via quantum illumination, *Science* **321**, 1463 (2008).
- [14] S.-H. Tan, B. I. Erkmen, V. Giovannetti, S. Guha, S. Lloyd, L. Maccone, S. Pirandola, and J. H. Shapiro, Quantum Illumination with Gaussian States, *Phys. Rev. Lett.* **101**, 253601 (2008).
- [15] S. Barzanjeh, S. Guha, C. Weedbrook, D. Vitali, J. H. Shapiro, and S. Pirandola, Microwave Quantum Illumination, *Phys. Rev. Lett.* **114**, 080503 (2015).
- [16] C. W. Sandbo Chang, A. M. Vadiraj, J. Bourassa, B. Balaji, and C. M. Wilson, Quantum-enhanced noise radar, *Appl. Phys. Lett.* **114**, 112601 (2019).
- [17] S. Barzanjeh, S. Pirandola, D. Vitali, and J. M. Fink, Experimental microwave quantum illumination, [arXiv:1908.03058](https://arxiv.org/abs/1908.03058).
- [18] E. Flurin, N. Roch, F. Mallet, M. H. Devoret, and B. Huard, Generating Entangled Microwave Radiation Over Two Transmission Lines, *Phys. Rev. Lett.* **109**, 183901 (2012).
- [19] C. Eichler, C. Lang, J. M. Fink, J. Govenius, S. Filipp, and A. Wallraff, Observation of Entanglement between Itinerant Microwave Photons and a Superconducting Qubit, *Phys. Rev. Lett.* **109**, 240501 (2012).
- [20] E. Flurin, N. Roch, J. D. Pillet, F. Mallet, and B. Huard, Superconducting Quantum Node for Entanglement and Storage of Microwave Radiation, *Phys. Rev. Lett.* **114**, 090503 (2015).
- [21] C. W. Sandbo Chang, M. Simoen, J. Aumentado, C. Sabín, P. Forn-Díaz, A. M. Vadiraj, F. Quijandría, G. Johansson, I. Fuentes, and C. M. Wilson, Generating Multimode Entangled Microwaves with a Superconducting Parametric Cavity, *Phys. Rev. Appl.* **10**, 044019 (2018).
- [22] X. Jia, X. Su, Q. Pan, J. Gao, C. Xie, and K. Peng, Experimental Demonstration of Unconditional Entanglement Swapping for Continuous Variables, *Phys. Rev. Lett.* **93**, 250503 (2004).
- [23] N. Takei, H. Yonezawa, T. Aoki, and A. Furusawa, High-Fidelity Teleportation Beyond the No-Cloning Limit and Entanglement Swapping for Continuous Variables, *Phys. Rev. Lett.* **94**, 220502 (2005).
- [24] S. Pirandola, D. Vitali, P. Tombesi, and S. Lloyd, Macroscopic Entanglement by Entanglement Swapping, *Phys. Rev. Lett.* **97**, 150403 (2006).
- [25] Q.-C. Sun, Y.-F. Jiang, Y.-L. Mao, L.-X. You, W. Zhang, W.-J. Zhang, X. Jiang, T.-Y. Chen, H. Li, Y.-D. Huang, X.-F. Chen, Z. Wang, J. Fan, Q. Zhang, and J.-W. Pan, Entanglement swapping over 100 km optical fiber with independent entangled photon-pair sources, *Optica* **4**, 1214 (2017).
- [26] J. Bochmann, A. Vainsencher, D. D. Awschalom, and A. N. Cleland, Nanomechanical coupling between microwave and optical photons, *Nat. Phys.* **9**, 712 (2013).
- [27] K. C. Balram, M. I. Davano, J. D. Song, and K. Srinivasan, Coherent coupling between radiofrequency, optical and acoustic waves in piezo-optomechanical circuits, *Nat. Photonics* **10**, 346 (2016).
- [28] L. Midolo, A. Schliesser, and A. Fiore, Nano-opto-electro-mechanical systems, *Nat. Nano.* **13**, 11 (2018).
- [29] D. Vitali, P. Tombesi, M. J. Woolley, A. C. Doherty, and G. J. Milburn, Entangling a nanomechanical resonator and a superconducting microwave cavity, *Phys. Rev. A* **76**, 042336 (2007).
- [30] C. Genes, A. Mari, P. Tombesi, and D. Vitali, Robust entanglement of a micromechanical resonator with output optical fields, *Phys. Rev. A* **78**, 032316 (2008).
- [31] S. Barzanjeh, D. Vitali, P. Tombesi, and G. J. Milburn, Entangling optical and microwave cavity modes by means of a nanomechanical resonator, *Phys. Rev. A* **84**, 042342 (2011).
- [32] V. Giovannetti and D. Vitali, Phase-noise measurement in a cavity with a movable mirror undergoing quantum Brownian motion, *Phys. Rev. A* **63**, 023812 (2001).
- [33] C. K. Law, Interaction between a moving mirror and radiation pressure: A Hamiltonian formulation, *Phys. Rev. A* **51**, 2537 (1995).
- [34] R. Benguria and M. Kac, Quantum Langevin Equation, *Phys. Rev. Lett.* **46**, 1 (1981).
- [35] I. S. Gradshteyn and I. M. Ryzhik, in *Table of Integrals, Series and Products* (Academic, Orlando, 1980), p. 1119.
- [36] P. C. Parks and V. Hahn, *Stability Theory* (Prentice-Hall, New York, 1993).
- [37] G. Vidal and R. F. Werner, Computable measure of entanglement, *Phys. Rev. A* **65**, 032314 (2002).
- [38] G. Adesso, A. Serafini, and F. Illuminati, Extremal entanglement and mixedness in continuous variable systems, *Phys. Rev. A* **70**, 022318 (2004).
- [39] J. D. Teufel, Dale Li, M. S. Allman, K. Cicak, A. J. Sirois, J. D. Whittaker, and R. W. Simmonds, Circuit cavity electromechanics in the strong-coupling regime, *Nature (London)* **471**, 204 (2011).
- [40] R. W. Andrews, R. W. Peterson, T. P. Purdy, K. Cicak, R. W. Simmonds, C. A. Regal, and K. W. Lehnert, Bidirectional and efficient conversion between microwave and optical light, *Nat. Phys.* **10**, 321 (2014).
- [41] M. Paternostro, D. Vitali, S. Gigan, M. S. Kim, C. Brukner, J. Eisert, and M. Aspelmeyer, Creating and Probing Multipartite Macroscopic Entanglement with Light, *Phys. Rev. Lett.* **99**, 250401 (2007).
- [42] D. Vitali, S. Gigan, A. Ferreira, H. R. Bhm, P. Tombesi, A. Guerreiro, V. Vedral, A. Zeilinger, and M. Aspelmeyer, Optomechanical Entanglement between a Movable Mirror and a Cavity Field, *Phys. Rev. Lett.* **98**, 030405 (2007).
- [43] C. Genes, D. Vitali, and P. Tombesi, Emergence of atom-light-mirror entanglement inside an optical cavity, *Phys. Rev. A* **77**, 050307(R) (2008).